Journal of Magnetic Resonance **151,** 78–84 (2001)
doi:10.1006/jmre.2001.2342, available online at http://www.idealibrary.com on IDEAL®

Longitudinally Detected EPR: Improved Instrumentation and New Pulse Schemes

Josef Granwehr, Jörg Forrer, and Arthur Schweiger

Physical Chemistry Laboratory, ETH Zentrum, CH-8092 Zürich, Switzerland
E-mail: granwehr@phys.chem.ethz.ch, forrer@phys.chem.ethz.ch, schweiger@phys.chem.ethz.ch

Received November 28, 2000; published online May 18, 2001

A new setup for longitudinal detection (LOD) of EPR signals based on a commercial pulse EPR spectrometer equipped with an ENDOR probehead is presented. The design is suited for pulse LOD EPR and amplitude-modulated cw LOD EPR experiments. The sensitivity is substantially increased compared with earlier designs. Two new pulse schemes that take full advantage of the special properties of the setup are invented. In *t*ransient-*n*utation *lo*ngitudinally *d*etected EPR (TN-LOD EPR), the nutation of magnetization during a microwave pulse is used to measure the EPR signal. In *p*ulse-*t*rain excited *lo*ngitudinally *d*etected EPR (PT-LOD EPR), a train of microwave pulses that periodically inverts the magnetization is applied. First experimental results on radicals and metal complexes at room temperature are presented.

Key Words: **electron spin resonance; pulse EPR; amplitude-modulated cw EPR; longitudinal detection; resonant circuit.**

INTRODUCTION

With longitudinal detection (LOD) the EPR signal is measured via the change in M_z magnetization, which induces a voltage in a pick-up coil oriented parallel to the static magnetic field $\mathbf{B}_0$. Such experiments have been carried out with continuous wave (cw) and pulse excitation for many years (*1–6*). The LOD technique is a useful alternative and supplement to the much more common detection of transverse magnetization. LOD EPR has successfully been used, for example, to measure longitudinal relaxation times (*7, 8*), to investigate slow dynamics effects (*9*), and to disentangle overlapped EPR spectra (*10, 11*). In recent years the LOD method has also extensively been applied in EPR imaging (*12–14*). However, up to now the technique has not found widespread applications in routine EPR spectroscopy, mainly because of its low sensitivity and the requirement of a dedicated spectrometer to perform the experiments.

In this work we present an experimental setup for LOD experiments that is based on a commercial pulse EPR spectrometer and that requires a minimum of additional equipment. The detection system is optimized to an extent that allows one to perform LOD EPR experiments with measuring times comparable to conventional cw EPR.

Two new pulse schemes that cause the M_z magnetization to oscillate with a frequency of several megahertz are introduced. In the first approach, called *t*ransient-*n*utation *lo*ngitudinally *d*etected EPR (TN-LOD EPR), either transient nutations or the periodic inversion of the magnetization is detected, depending on the relaxation time of the paramagnetic species. The second approach, called *p*ulse-*t*rain *lo*ngitudinally *d*etected EPR (PT-LOD EPR), detects the change of the M_z magnetization induced by a train of pulses, and is related to a method that has previously been developed for much lower pulse repetition frequencies (*4*).

The potential of the new experimental setup and of the two pulse schemes is demonstrated on a coal sample and on transition metal complexes.

LOD EPR EXPERIMENTS

In this section we briefly summarize the basics of cw LOD EPR and introduce the new pulse LOD EPR schemes.

The cw LOD Experiment

Continuous wave LOD EPR experiments can be carried out by using a microwave (mw) field that is amplitude-modulated either with frequency ω when a carrier is present (*15*) or with frequency $\omega/2$ with suppressed carrier. The second case is equivalent to the irradiation of two mw fields that differ in frequency by ω (*3*). Both experiments cause the M_z magnetization to oscillate with the frequencies $n\omega$, where $n = 1, 2, \ldots$. The LOD experiments can be described using Bloch equations (*7, 16*) or second quantization (*17*). For two frequencies and $\omega^{-1} \gg T_1$ it has been shown by using Bloch equations that the response from the spin system has nonvanishing Fourier components for $n \geq 1$ (*16*). Detection is done by tuning the resonant frequency ω_{LCR} of the detection circuit to one of these frequencies, usually to ω.

The lineshapes of a cw LOD EPR spectrum may be distorted for various reasons. We mention here only the two most relevant mechanisms. The first one is comparable to power broadening in cw EPR. If the mw power exceeds a certain level, a homogeneous EPR line will split into a doublet. For $\omega^{-1} \gg T_1$ and detection of the fundamental frequency $\omega_{\mathrm{LCR}} = \omega$, such

1090-7807/01 $35.00

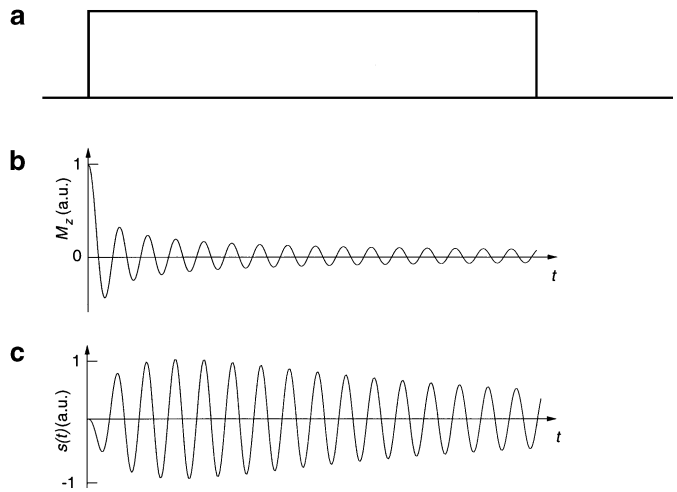

FIG. 1. TN-LOD EPR experiment. (a) Pulse sequence consisting of a single strong mw pulse. (b) Nutating M_z magnetization of a spin system with a homogeneous EPR line. The decay is caused by a distribution of the mw field strength ω_1. (c) Response of the resonant circuit with quality factor $Q_{\mathrm{LCR}} = 10$.

a splitting is observed for $S > 2(1+\sqrt{2}) = 4.828$ (*16*), where $S = (\gamma B_1)^2 T_1 T_2$ is the saturation parameter (*18*). The splitting occurs readily for radicals with long relaxation times, whereas for transition metal complexes at room temperature, line broadenings or line splittings are not observed even at the maximum available mw power. The second mechanism for line distortions is independent of B_1. A splitting of the EPR lines can be observed if the linewidths are narrower than ω because the sidebands of the mw radiation lie outside the EPR lines.

Transient-Nutation LOD EPR

In the TN-LOD EPR experiment shown in Fig. 1, the M_z magnetization nutates under the influence of a strong mw pulse and induces a voltage in the pick-up coil. The nutation frequency ω_{TN} is proportional to the product of the transition matrix element of the excited transition and the field strength B_1 and depends on the resonance offset and on the magnetic parameters of the spin system (*19–21*). For example, the magnetization vector in a spin system with $S = 1/2$ and an isotropic g value nutates with frequency

$$\omega_{\mathrm{TN}} = \sqrt{\omega_1^2 + \Omega_S^2}, \qquad [1]$$

where $\Omega_S = \beta_e g B_0/\hbar - \omega_{\mathrm{mw}}$ is the resonance offset and $\omega_1 = \beta_e g B_1/\hbar$ is the mw field strength in angular frequency units.

Since in our experiments a detection circuit with a narrow bandwidth and a resonance frequency ω_{LCR} is used, ω_{TN} must be adjusted to ω_{LCR} by varying B_1. For $\omega_1 < \omega_{\mathrm{LCR}}$, the condition $\omega_{\mathrm{TN}} = \omega_{\mathrm{LCR}}$ is fulfilled at the off-resonant field positions $\Omega_S = \pm\sqrt{\omega_{\mathrm{LCR}}^2 - \omega_1^2}$. Narrow EPR lines with a width on the order of ω_{LCR} or smaller may thus be split into two peaks separated by $2\sqrt{\omega_{\mathrm{LCR}}^2 - \omega_1^2}$. For $\omega_1 > \omega_{\mathrm{LCR}}$ the signal intensity is reduced and the lines are broadened. A similar ω_1 dependence is found for paramagnetic species with anisotropic **g** matrices or $S > \frac{1}{2}$.

To illustrate the characteristics of the experiment we use a numerical simulation procedure based on the GAMMA library (*22*), and assume an $S = \frac{1}{2}$ system with a homogeneously broadened line, on-resonant mw irradiation, and a distribution of the ω_1 values typical for dielectric resonators and large samples (*21*). T_1, T_2 are chosen much larger than $\omega_{\mathrm{LCR}}^{-1}$. The resulting signal depends strongly on the properties of the resonant circuit. Figures 1b and 1c show the time evolution of $M_z(t)$ and the signal $s(t)$ in a serial LCR resonant circuit with ω_{LCR} equal to the maximum of the ω_1 distribution.

The field-swept TN-LOD EPR spectrum is obtained either by Fourier transformation of $s(t)$ at each B_0-field position and taking the spectral component at ω_{LCR}, or by multiplying $s(t)$ with a reference signal of frequency ω_{LCR} and taking the spectral component at zero frequency. As a third possibility for samples with strong signals, the data points of $|s(t)|$ can be summed up after a baseline correction for each position of B_0.

The decay of the magnetization caused by off-resonance contributions and B_1-field inhomogeneities can be partially refocused to a rotary echo (*20*) by changing the phase of the mw field by 180°. This procedure can be repeated several times resulting in the pulse sequence shown in Fig. 2a, with a first nutation pulse of length t_{p} followed by a succession of refocusing pulses with alternating phases and length $2t_{\mathrm{p}}$. Since for detection the phase of the oscillating magnetization must remain the same during the whole pulse sequence, t_{p} must be set to

$$t_{\mathrm{p}} = \frac{n}{2}\frac{2\pi}{\omega_{\mathrm{LCR}}}, \quad n = 1, 2, \ldots. \qquad [2]$$

Figure 2b shows the evolution of M_z for the scheme with refocused magnetization. The same distribution of ω_1 and the same values for T_1, T_2 as in Fig. 1 have been used. The magnetization is completely refocused since in this simulation a

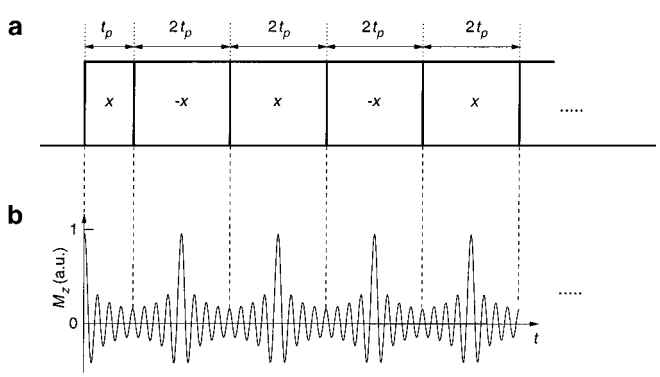

FIG. 2. TN-LOD EPR experiment with refocused magnetization and the same ω_1 distribution as described in the legend to Fig. 1. (a) Pulse sequence consisting of an mw pulse that is subdivided into segments with alternating phases to generate a train of rotary echoes. (b) Time evolution of M_z for a spin system with a homogeneous EPR line in an inhomogeneous mw field.

homogeneous EPR line with on-resonant mw irradiation is assumed.

For $T_2 \ll 2\pi/\omega_{LCR}$, the spin system behaves completely different. The nutation is overdamped and M_z approaches a steady state during the mw pulse. In this case the magnetization can not be refocused, and the spin system behaves as in a cw LOD experiment with phase modulation of the mw field. Without phase modulation, the resonant circuit is excited twice. The first time by the rapid approach of M_z to a steady state when the pulse is switched on, and the second time by the fast return of M_z to the Boltzmann equilibrium when the pulse is switched off. If the duration of the mw pulse is a half-integer multiple of the period of the resonant circuit, the two signals are added; if the length is an integer multiple, the signals are subtracted.

TN-LOD EPR is particularly well suited for transition metal complexes at liquid helium temperature and for radicals at room temperature where the nutation of the magnetization lasts for several periods. It can also successfully be applied in cases where the spectrum consists of both broad and narrow lines because, as aforementioned, different mechanisms are responsible for the signal, depending on whether nutation lasts for a long or a short time.

Pulse-Train LOD EPR

The PT-LOD EPR experiment consists of a train of mw pulses of length t_p, separated by the repetition time t_{rep} (Fig. 3a). Such an excitation scheme has already been used for LOD experiments with pulse repetition frequencies $1/t_{rep}$ between 1 and 10 kHz and $t_{rep} \gg t_p$(*4*). In this earlier approach the sequence consisted of an infinite number of π pulses, and the resonant circuit with frequency $\omega_{LCR} = 2\pi/t_{rep}$ filtered the first Fourier component of the periodically changing z magnetization. The sinusoidal signal was recorded with a phase-sensitive detector (PSD). In the approach proposed here, a pulse repetition frequency of about 10 MHz is used and t_{rep} and t_p are of the same order of magnitude. This corresponds to an increase of the detection frequency by three to four orders of magnitude compared to the former scheme, and the signal intensity is concentrated on the fundamental frequency and a few higher harmonics. In contrast to the low-frequency approach detection is done with a transient recorder, since the length of the pulse train is limited by the duty cycle of the TWT amplifier.

As in the TN-LOD EPR experiment the signal observed in the PT-LOD experiment strongly depends on the effect of the mw pulses on the spin system, i.e., whether the magnetization can be inverted several times with strong mw pulses. These two cases will be discussed separately.

No inversion of the magnetization possible ($T_2 \ll 2\pi/\omega_{LCR}$). In this case the magnetization approaches its steady-state value during each pulse and partially recovers between the pulses. This is shown in Fig. 3b for $t_{rep} = 2t_p$. The pulse repetition time must

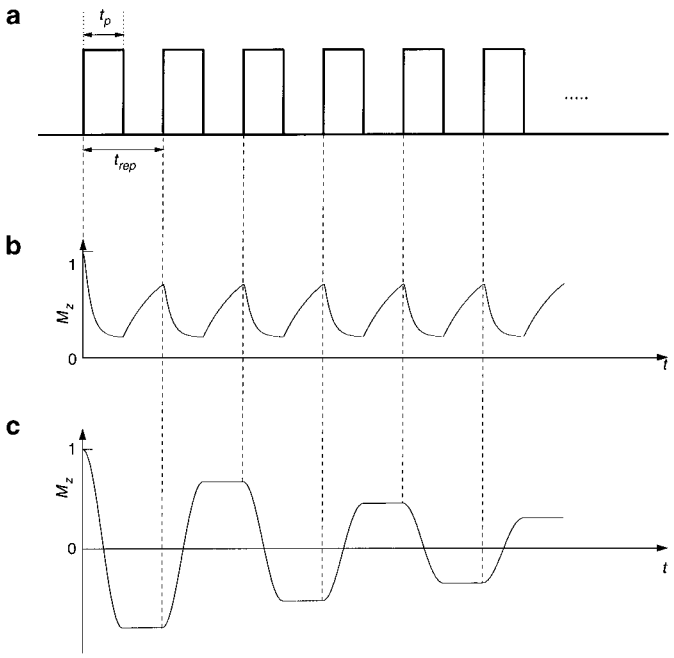

FIG. 3. PT-LOD EPR experiment. (a) Pulse sequence consisting of a train of π pulses of length t_p and a pulse repetition time $t_{rep} = 2t_p$. (b) Behavior of the M_z magnetization for the case $T_2 \ll 2\pi/\omega_{LCR}$. Parameters used for the simulation are as follows: $t_{rep} = 80$ ns, $T_1 = 40$ ns, $T_2 = 1$ ns. (c) Behavior of the M_z magnetization for the case $T_1 \gg 2\pi/\omega_{LCR}$ and T_2 on the order of $2\pi/\omega_{LCR}$. The pulse sequence inverts the magnetization periodically (parameters: $T_1 = 40\ \mu$s, $T_2 = 100$ ns).

be set to

$$t_{rep} = 2\pi n/\omega_{LCR}, \qquad [3]$$

where n is a positive integer; otherwise the signals induced by the different pulse do not have the same phase, which reduces the detected signal. After a few cycles, the magnetization reaches an oscillatory steady state. If $n = 1$, the time constant of the detection circuit is not only responsible for the ringing after the pulse train, but also for the rise of the signal during excitation. In the limit of a pulse train with an infinite number of pulses and for $t_{rep} = 2t_p$, the only difference between this method and the cw LOD experiment with a square-wave modulation of the mw field amplitude is to use a transient recorder instead of a PSD for detection.

At least partial inversion of magnetization possible, and $T_1 \gg t_{rep}$. In this case $M_z(t)$ remains virtually unchanged between two consecutive pulses, so that the maximum signal is obtained with flip angles of 180° (Fig. 3c). The decay of the magnetization caused by the inhomogeneous B_1 field and inhomogeneous EPR lines can partially be refocused by alternatingly inverting the phase of the pulses. The change in M_z is thus periodic with $2t_{rep}$, and a repetition time $t_{rep} = \pi/\omega_{LCR}$ must be used for maximum signal intensity. The signal $s(t)$ will first increase and then slowly decrease to a low steady-state value. Lines with a

width smaller than the excitation bandwidth of the pulses will be broadened. For optimum signal intensity, the same rules apply for the choice of the repetition time between two pulse trains as in pulse echo experiments (*18*).

INSTRUMENTATION

Spectrometer

The setup for the LOD experiments is integrated in a Bruker ELEXSYS E580 pulse/cw EPR spectrometer operating at X-band frequencies (Fig. 4). Two separate channels are used for pulse LOD and cw LOD experiments, both for excitation and detection.

Pulse mode. For pulse LOD experiments, a modification of the excitation channel is not required. The mw pulses are formed in the mw bridge of the E580 spectrometer and amplified up to 1 kW with a TWT with a duty cycle of 1%. For data acquisition the preamplified signal is fed to the Bruker SpecJet transient signal averager, which is the built-in device for data acquisition.

Continuous wave mode. To perform cw LOD experiments, the spectrometer must be supplemented by additional devices. The cw mw power is taken from the *AUX* output of the mw bridge. Its amplitude is modulated either with an mw switch (M/A-Com 2662-0106) for square-wave modulation, or with a double balanced mixer (Miteq MO 812) for arbitrary modulations. Amplitude modulation of the mw is by far less demanding than the use of two frequency-locked mw sources (*3*). The modulated signal is then amplified with a 15-W solid state cw mw amplifier (CTT ASN 096-4242). The power level at the output of the mw amplifier is adjusted by a rotary vane attenuator (Sivers Lab PM 7101X). The isolators are used to generate an mw amplitude modulation free of reflections (Ryt 200102) and to absorb reflections caused by the overcoupling of the probehead (Narda 60583). The signal from the pick-up coil is amplified and demodulated with a phase-sensitive detector (Stanford SR 844). The signal output of this device is then directed to the Spec-Jet. The driving signal for the mw modulators is delivered by an arbitrary waveform generator (LeCroy LW 420) and is also used as reference for the PSD.

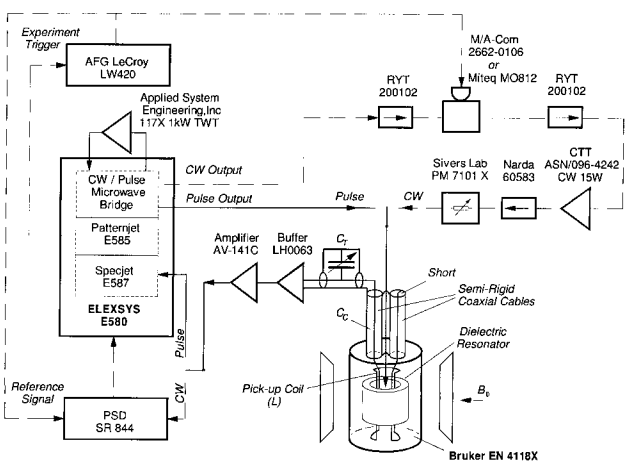

FIG. 4. Experimental setup used for LOD EPR experiments based on a Bruker ELEXSYS E580 pulse EPR spectrometer with a pulse ENDOR probehead rotated by 90° around the sample axis. The parts connected by dashed lines are used for cw LOD EPR only.

Probehead

Dielectric resonators are well suited for both pulse and cw EPR experiments. Their loaded quality factors Q_L can be adjusted between 80 (maximal overcoupled with power reflection of approximately 99%) and 5000 (critical coupling). Furthermore, a coil positioned inside the dielectric ring close to the sample has only a small influence on the mw properties of this type of resonator.

As LOD experiments usually suffer from sensitivity, the design of the pick-up coil must be optimized carefully. The voltage

$$V_{ind} \propto -NA\frac{dM_z(t)}{dt} \qquad [4]$$

induced in a coil by the time-dependent M_z magnetization is proportional to the number N of turns and to the cross section A of the coil. For optimum sensitivity, the coil should have a maximum number of turns and should be as close to the sample as possible. On the other hand, N is limited by the maximum inductance L of the coil for a given resonance frequency ω_{LCR} and the available space, and the wires must be arranged such that they are oriented perpendicular to the electric field component of the mw field.

The setup of the Bruker X-band probehead (EN 4118X) for ENDOR experiments fulfills most of the above requirements. The wire of the radio frequency (rf) coil is guided inside the dielectric ring in four grooves parallel to the sample axis and returns outside the dielectric body. The coil is thus very close to the sample with 3.8-mm outer diameter, resulting in a much higher filling factor than in all coil arrangements previously used for LOD experiments. We performed our LOD experiments with such a commercial probehead, rotated around the sample axis by 90°, and used the rf coil, which is then oriented parallel to $\mathbf{B}_0$, as the pick-up coil.

For pulse LOD experiments, the resonator was strongly overcoupled to obtain well-defined pulse shapes. For cw LOD experiments the quality factor Q_L must be chosen such that the bandwidth of the resonator ω_{mw}/Q_L is larger than the frequency difference between the mw sidebands. Otherwise the signal intensity is remarkably reduced. In addition, the two sidebands may have different intensities if mw and resonator frequency are not the same.

Detection Circuit

The LOD detection setup, which can be described best as a serial LCR resonant circuit, requires only a minimum of additional devices. The rf coil of the ENDOR probehead with an

inductance $L \approx 2.6\ \mu$H is used for signal detection. One of the two semi-rigid 50-Ω coaxial cables that connect this coil with the rf connectors at the outside of the probehead is shorted. This connection, which adds an inductive part with $L_C \approx 0.15\ \mu$H, is not considered in the following. The second semi-rigid coaxial cable has a high-impedance termination and acts therefore as a capacitor with $C_C \approx 50$ pF between coil and ground. These components of the probehead already form a serial LCR resonant circuit with a resonance frequency $\omega_{\mathrm{LCR}}/2\pi = 1/(2\pi\sqrt{LC}) \approx$ 14 MHz and a quality factor $Q_{\mathrm{LCR}} = R_S^{-1}\sqrt{L/C} \approx 150$. The resistance of the coil represents the main contribution to the serial resistance R_{S}. In going from room temperature to liquid helium temperature, Q_{LCR} increases by a factor 2–3. If the first semi-rigid coaxial cable is open ended, ω_{LCR} increases by about a factor $\sqrt{2}$. To adjust the resonance frequency of the detection circuit, a tuning capacitor with $C_T = 5$–15 pF in parallel to C_C is used. The signal is detected as the voltage across capacitance $C = C_C + C_T$. The impedance transformation between the resonant circuit and the 50-Ω input of the rf preamplifier (Avtec AV-141C) is realized with a buffer amplifier (National LH0063). The advantage of this active transformation over a passive one is that Q_{LCR} is not reduced by the transformed input impedance of the video amplifier.

The S/N ratio of the detection system can be expressed by (*23–25*)

$$S/N \propto M_0\sqrt{\eta Q_{\mathrm{LCR}}\frac{\omega_{\mathrm{LCR}}}{\Omega_{\mathrm{b}}}\frac{V_{\mathrm{S}}}{FT_0}}, \qquad [5]$$

where η is the filling factor of the detection coil, V_{S} is the sample volume, Ω_{b} is the bandwidth of the receiver, F is the noise figure of the preamplifier, and T_0 is the temperature of the detection coil. With the setup used in this work, the sensitivity is particularly high because of the high η value and the high resonant frequency $\omega_{\mathrm{LCR}}/2\pi \approx 13$ MHz, which is three orders of magnitude higher than in earlier pulse LOD work (*4*). In cw LOD, detection frequencies up to 30 MHz have been used (*7*).

RESULTS AND DISCUSSION

In this section we illustrate the potential of the various LOD techniques by experimental examples. All spectra were recorded at room temperature with a resonance frequency $\omega_{\mathrm{LCR}}/2\pi =$ 12.5 MHz.

For the pulse LOD experiments, the window for the transient signal detection was opened at the beginning of the pulse sequence and its length was set so that also the first part of the ringing of the detection circuit after the end of the excitation was recorded. Real-time data analysis is not possible with the spectrometer software used in this work. Optimization of the various instrumental parameters, such as mw attenuation, mw phases, and lengths of the pulses and of the detection window, can be done in real-time by observing the signal on the oscilloscope.

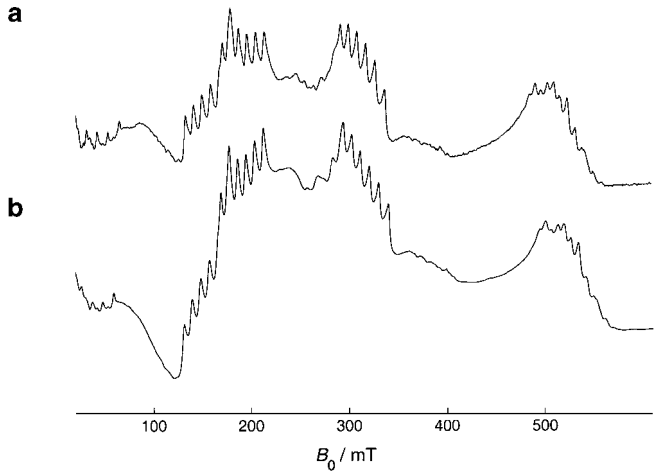

FIG. 5. Continuous wave LOD EPR experiment. (a) LOD EPR spectrum of a powder of Mn-doped NH_4Cl recorded at room temperature with a square-wave modulated mw amplitude (mw frequency 9.6303 GHz). (b) Corresponding integrated cw EPR spectrum (mw frequency, 9.7686 GHz).

cw LOD EPR

The cw LOD powder EPR spectrum of Mn(II)-doped NH_4Cl (0.08%) (*26*) recorded with a square-wave modulated mw field is shown in Fig. 5a. The quality factor of the mw resonator was $Q_{\mathrm{L}} = 700$ and the mw power was 5 W. The spectrum with a S/N ratio of about 120 was measured in 2 min. with a resolution of 1024 data points. For comparison, the integrated cw EPR spectrum is shown in Fig. 5b. It is difficult to get the correct baseline for a cw EPR spectrum that covers such a wide field range. For cw LOD EPR the linewidth and the width of the spectrum represent no limitations since the absorption spectrum instead of its first derivative is detected. The small shift in the field axis of the two spectra is caused by the use of two slightly different mw frequencies.

Since in this setup the pick-up coil is placed inside the resonator, spurious lines from paramagnetic impurities in the dielectric ring do not disturb the spectrum. This is often a problem in cw EPR experiments using this type of resonator.

TN-LOD EPR

In Fig. 6 TN-LOD EPR spectra of a coal sample with a narrow radical signal and a broad signal from an iron impurity recorded without (6a) and with (6b) refocusing of the magnetization are compared with the integrated cw EPR spectrum (6c). The TN-LOD spectra were recorded in 10 min. with a resolution of 601 data points. Three minutes of the recording time were used for data acquisition; the rest was instrumental overhead to transfer the data to the computer and to reset the pulse programmer. All TN-LOD and PT-LOD experiments suffered from such an overhead, which was almost zero in the cw LOD experiments. The nutation frequency resonant with the radical peak was adjusted to ω_{LCR} by varying the mw power until the signal was maximum.

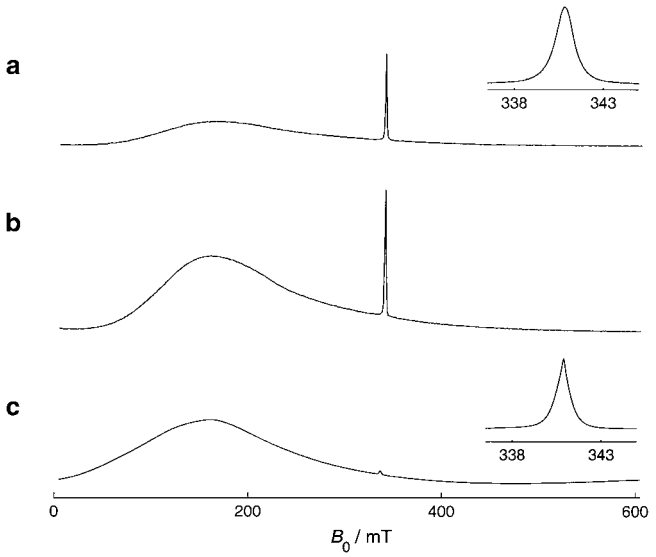

FIG. 6. TN-LOD EPR experiment. (a) TN-LOD EPR spectrum of a coal sample recorded without refocusing of the magnetization. The length of the mw pulse was 1 μs. (b) TN-LOD EPR spectrum recorded with refocusing of the magnetization. The pulse consists of one segment of length $t_p = 160$ ns and eight segments of length $2t_p$. (c) Integrated cw EPR spectrum, recorded with a modulation amplitude of 2.3 mT for the full spectrum and 0.1 mT for the inset.

The sensitivity of this adjustment procedure can be increased by periodically changing the phase of the mw field by 180°, which generates a train of rotary echoes. The time between the echoes should be equal to one or two periods of the resonant circuit.

Since the relaxation time of the iron spectrum is short compared to a nutation period, the phase switching acts as a phase modulation, which increases the signal intensity. Therefore the iron spectrum in Fig. 6a is three times weaker in intensity than in the corresponding spectrum in Fig. 6b. An S/N ratio of 40 is found for the iron spectrum in 6a and of 130 in 6b. The inset in 6a, which represents the spectrum of the radical with an S/N ratio of 170 and a resolution of 256 points, was recorded in 4 min. For the cw EPR spectrum shown in 6c a modulation amplitude of 2.3 mT (inset: 0.1 mT) and an mw power of 0.2 W (inset: 20 μW) were used.

The spectrum of the radical is different in the TN-LOD EPR and the cw EPR experiments, since this sample contains several radical components with different linewidths. For the radical with the small linewidth, one finds $T_1 \approx T_2$, which is a favorable condition for the detection of field-modulated cw EPR spectra, especially with the low mw power used in this measurement. Therefore the relative intensity of the narrow line compared to the broad line is larger in the conventional cw EPR spectrum than in the TN-LOD EPR spectrum, where the contribution of the narrower line to the signal is small. With an echo-detected EPR experiment at room temperature almost the same result as with the TN-LOD EPR was obtained since from the narrow line only an FID but no echo could be observed.

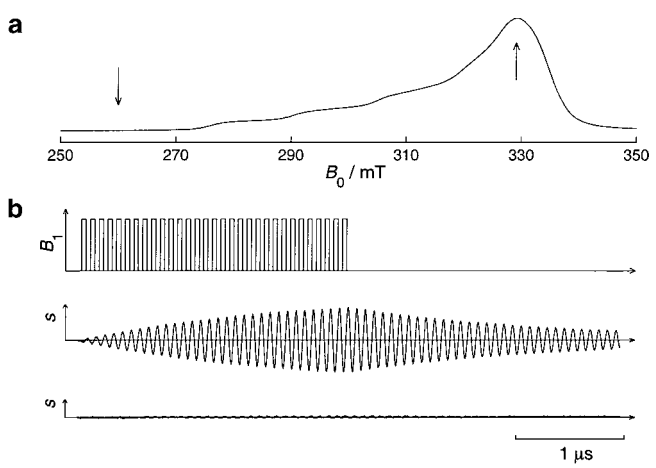

FIG. 7. PT-LOD EPR experiment. (a) PT-LOD powder EPR spectrum of bis(picolinato)Cu(II) diluted into the corresponding zinc complex. The two arrows indicate the B_0-field observer positions used for the time traces in (b). (b) Pulse sequence consisting of 31 mw pulses (top). PT-LOD time trace recorded with an observer field of 329 mT (middle). Corresponding off-resonance signal recorded at 260 mT (bottom).

PT-LOD EPR

Figure 7a shows the PT-LOD EPR spectrum of bis(picolinato) Cu(II) doped into a powder of the corresponding zinc complex. The spectrum with an S/N ratio of 350 was measured with 500 data points in 8 min. and was obtained by a train of 31 mw pulses of length 40 ns (Fig. 7b (top)). An mw power of 150 W and a pulse repetition time $t_{rep} = 80$ ns were used. The time-domain trace observed by adding 100 shots at the B_0-field position where the EPR signal is maximum is shown in Fig. 7b (middle, arrow in 7a at the high-field position) together with the residual signal observed with an off-resonance field (bottom, arrow in 7a at the low-field position).

CONCLUSIONS

We described a setup for longitudinally detected EPR at X-band frequencies that overcomes some of the shortcomings of earlier approaches and that is sufficiently sensitive to perform routine measurements. The same probehead can be used for pulse LOD EPR and amplitude-modulated cw LOD EPR experiments. Since a commercially available probehead initially designed for pulse ENDOR experiments was used without modifications, the sensitivity may be improved further by optimizing the probehead for this type of experiments. A probehead where the whole resonant circuit including the impedance matching network and the preamplifier are at cryogenic temperatures could fully benefit from the low value of T_0 and the high Q_{LCR} value (see Eq. [5]), since no noise source at ambient temperature is part of the detection circuit.

The two new pulse schemes, TN-LOD EPR and PT-LOD EPR, require fast accumulation of transient signals, a technique

that has recently become available. TN-LOD EPR is well suited for the measurement of EPR spectra with both narrow and broad lines. On the other hand, the proper recording of the spectrum and the optimum choice of the different parameters that depend on the type of sample under investigation can be quite demanding. PT-LOD EPR is easier to implement because the adjustment of the mw power is less critical. The approach is most sensitive for paramagnetic species with T_1 on the order of or shorter than an oscillation period of the detection circuit. For paramagnetic species with linewidths smaller than the excitation bandwidth of the pulses, the signals may be broadened and distorted. In the two pulse LOD EPR methods the whole time trace of the signal is recorded. It is therefore in principle possible to calculate the evolution of $M_z(t)$ and to obtain additional information about the spin system, provided the parameters of the resonant circuit are known.

Since several properties of LOD EPR are complementary to conventional cw EPR, longitudinal detection can foster the interpretation of complicated spectra by comparing the spectra obtained with the two detection methods. Another important application of LOD techniques, which is not discussed in detail in this work, is the measurement of spin–lattice relaxation times T_1. The setup described in this work opens the possibility for new pulse LOD schemes for the determination of T_1 in a wide time window (27). The LOD EPR experiments discussed in this work require only some standard additional electronic components and can easily be implemented in existing spectrometers even without the need to build a dedicated probehead. Longitudinally detected EPR has thus become available for many laboratories.

ACKNOWLEDGMENTS

This work has been supported by the Swiss National Science Foundation. We thank the electronic group of our laboratory for many helpful advices concerning the optimization of the experimental setup. Furthermore, we are grateful to Dr. J. Harmer for providing us with the coal sample and to Dr. R. Bachmann for his first attempts to reinvestigate this field of EPR spectroscopy.

REFERENCES

1. N. Bloembergen and R. W. Damon, Relaxation effects in ferromagnetic resonance, *Phys. Rev.* **85,** 699 (1952).
2. G. Whitfield and A. G. Redfield, Paramagnetic resonance detection along the polarizing field direction, *Phys. Rev.* **106,** 918–920 (1957).
3. F. Chiarini, M. Martinelli, L. Pardi, and S. Santucci, Electron-spin double resonance by longitudinal detection: Line shape and many-quantum transitions, *Phys. Rev. B* **12,** 847–852 (1975).
4. A. Schweiger and R. R. Ernst, Pulsed ESR with longitudinal detection. A novel recording technique, *J. Magn. Reson.* **77,** 512–523 (1988).
5. H. Levanon, C. L. Kwan, and S. I. Weissman, Direct observation of growth of magnetization in excitation of triplet states, *Chem. Phys. Lett.* **6,** 19–20 (1970).
6. T. Sato, H. Yokoyama, H. Ohya, and H. Kamada, Measuring method of longitudinally detected ESR signal intensities against resonant frequencies at 250 to 950 MHz in a constant microwave field, *Appl. Magn. Reson.* **16,** 33–43 (1999).
7. J. Pescia, La mesure des temps de relaxation spin-réseau très courts, *Ann. Phys.* **10,** 389–406 (1965).
8. T. Strutz, A. M. Witowski, R. E. M. de Bekker, and P. Wyder, Pick-up coil as a tool of measuring spin-lattice relaxation under electron spin resonance condition at high magnetic fields, *Appl. Phys. Lett.* **57,** 831–833 (1990).
9. L. Andreozzi, M. Giordano, D. Leporini, M. Martinelli, and L. Pardi, Nonlinear electron paramagnetic resonance spectroscopy: Direct observation of slow dynamics effects at polymer glass transition, *Phys. Lett. A* **160,** 309–314 (1991).
10. G. Ablart, J. Pescia, S. Clement, and J. P. Renard, Experimental evidence of two overlapping paramagnetic species, *Solid State Commun*, **45,** 1027–1030 (1983).
11. M. Martinelli, L. Pardi, C. Pinzino, and S. Santucci, Dependence on relaxation times of longitudinally detected paramagnetic resonance, *Solid State Commun.* **17,** 211–212 (1975).
12. I. Nicholson, F. J. L. Robb, and D. J. Lurie, Imaging paramagnetic species using radiofrequency longitudinally detected ESR (LODESR Imaging), *J. Magn. Reson. B* **104,** 284–288 (1994).
13. H. Yokoyama, T. Sato, T. Ogata, H. Ohya-Nishiguchi, and H. Kamada, *In vivo* longitudinally detected ESR measurements at microwave regions of 300, 700, and 900 MHz in rats treated with a nitroxide radical, *J. Magn. Reson.* **129,** 201–206 (1997).
14. I. Nicholson, F. J. L. Robb, S. J. McCallum, A. Koptioug, and D. J. Lurie, Recent developments in combining LODESR imaging with proton NMR imaging, *Phys. Med. Biol.* **43,** 1851–1855 (1998).
15. J. Hervé and J. Pescia, Mesure du temps de relaxation T_1 par modulation du champ radiofréquence H_1 et détection de la variation d'aimanation selon le champ directeur, *C. R. Acad. Sci. (Paris)* **251,** 665–667 (1960).
16. J. J. Davies, On the longitudinal magnetization of a spin system subjected to double magnetic resonance, *Solid State Commun.* **20,** 433–435 (1976).
17. M. Martinelli, L. Pardi, C. Pinzino, and S. Santucci, Electron-spin double resonance by longitudinal detection. II. Signal dependence on relaxation times, *Phys. Rev. B* **16,** 164–169 (1977).
18. R. R. Ernst, G. Bodenhausen, and A. Wokaun, "Principles of Nuclear Magnetic Resonance in One and Two Dimensions," Clarendon Press, Oxford (1987).
19. A. V. Astashkin and A. Schweiger, Electron-spin transient nutation: A new approach to simplify the interpretation of EPR spectra, *Chem. Phys. Lett.* **174,** 595–602 (1990).
20. S. Stoll, G. Jeschke, M. Willer, and A. Schweiger, Nutation-frequency correlated EPR spectroscopy: The PEANUT experiment, *J. Magn. Reson.* **130,** 86–96 (1998).
21. S. Stoll, "Nutation-Correlated EPR Spectroscopy," Diploma Thesis, Physical Chemistry Laboratory, ETH Zürich (1996).
22. S. A. Smith, T. O. Levante, B. H. Meier, and R. R. Ernst, Computer simulations in magnetic resonance. An object oriented programming approach, *J. Magn. Reson. A* **106,** 75–105 (1994).
23. A. Abragam, "The Principles of Nuclear Magnetism," Clarendon Press, Oxford (1961).
24. D. I. Hoult and R. E. Richards, The signal-to-noise ratio of the nuclear magnetic resonance experiment, *J. Magn. Reson.* **24,** 71–85 (1976).
25. J. S. Hyde, P. B. Sczaniecki, and W. Froncisz, The Bruker lecture. Alternatives to field modulation in electron spin resonances spectroscopy. *J. Chem. Soc. Faraday Trans. I* **85,** 3901–3912 (1989).
26. R. Bramley and J. Strach, Improved spin Hamiltonian parameters for Mn^{2+} determined by EPR at zero magnetic field, *Chem. Phys. Lett.* **79,** 183–188 (1981).
27. J. Granwehr and A. Schweiger, Measurement of spin-lattice relaxation times with longitudinal detection, *Appl. Magn. Resou.* **20,** 137–150 (2001).